

Micro Mechanical Thin Film Structures Spring Constant Analysis and Design of Shunt Capacitive RF MEMS Switches

Mallikharjuna Rao Sathuluri^{1,2}, G. Sasikala¹

¹ECE Department, Vel Tech Rangarajan Dr. Sagunthala R&D Institute of Science and Technology (Deemed to be University), Avadi, Tamil Nadu, India.

²ECE Department, Andhra Loyola Institute of Engineering and Technology, Vijayawada, A.P, India.

ABSTRACT

In this communication, we are analyzed micro level mechanical thin film structures spring constant required for design of RF MEMS switches. Overall four structures i.e. Cantilever, Bridge, Clamped-Clamped flexure and Serpentine flexure are taken in to consideration. We observed that the cantilever and serpentine flexure structures are offering less actuation voltage and less switching time which is essential for the design of RF MEMS switches. Finally, we mounted a RF MEMS switch with a serpentine configuration on the CPW transmission line that provides very low pull-in voltage, and very high isolation. Along with the 1GHz-40GHz frequency range, the radio frequency properties of the switch are tested.

Key words: Spring Constant, Cantilevers, Resonant Frequency (RF).

1. INTRODUCTION

The demand on the micro mechanical structures in the design of present day digital and communication modules attracting the researchers to do the work on MEMS technology. From few decades onwards the research on MEMS technology is advanced, but still there are so many challenges for the researchers for optimization. Major applications of the MEMS technology are accelerometers, gyroscopes, RF Switches, RF filters, RF Phase Shifters, RF Isolators [1-5]. The performance of the MEMS technology based devices is decided by the parameters like spring constant, deformation speed, resonant frequency, structure mass, Structure fatigue nature, losses, actuation force, environmental effects [1].

The The key research of the authors is on RF MEMS

switches, so our research on the function of MEMS structures has been expanded to construct RF MEMS switches. The MEMS structure's spring constant is the key consideration that will determine the Eigen values of the switch, pull voltage, and switching direction[1-3]. The authors of this paper expanded the work on spring constant formulation for micro-level mechanical systems such as cantilever, bridge, clamped-clamped flexure, serpentine flexure[4-8].

2. MICRO LEVEL MECHANICAL STRUCTURES

The architecture of MEMS technology devices relies primarily on mechanical structures at the micro level that can be operated electrostatically (or) thermally (or) piezoelectrically (or) magnetostatically. Cantilevers, bridges, clamped-clamped flexure, serpentine flexure, crab leg flexure, folded flexure, are common MEMS structures. We also based on the composition of the the spring constant of these MEMS systems in this article. It is possible to transmit the force on a rigid body as [1],

$$F = m\ddot{\delta} + B\dot{\delta} + K\delta \quad (1)$$

Where, ' δ ' displacement after applying the force 'F', ' $\dot{\delta}$ ' first-order derivative of the velocity-giving displacement, ' $\ddot{\delta}$ ' second-order derivative of the accelerating displacement, 'm' frame mass, 'B' damping coefficient, and 'K' spring constant.

In this analysis the force on the MEMS structure is applied vertically, so the structure displaces vertically. These are the micro level structures we can neglect the mass and the damping factor i.e. the displacement is a constant factor, so the derivative of constant is zero. After neglecting the first two terms in Eq. 1, we can approximate the force on the structure is i.e., Hooke's Law [2],

$$F = K\delta \quad (2)$$

We may give the expression of the spring constant 'k' in N / m. It is the ratio between the power and the displacement of the spring.

$$K = \frac{F}{\delta} \tag{3}$$

$$F = \frac{QE_f}{2} = \frac{CVE_f}{2} = \frac{CV^2}{2} = \frac{\epsilon_r \epsilon_0 AV^2}{2g^2} \tag{4}$$

If the structure is a cantilever, the displacement (δ) function can be expressed as, after applying a force (F) as shown in Fig. 1 is given as [1]

$$\delta = \frac{Fl^3}{Ewt^3} \tag{5}$$

Where, the charge between the conductors is 'Q', 'E_f' electric field, 'C' capacitance, 'V' is the voltage applied, 'A' region over the electrodes, 'g' gap between the electrodes and $\delta_{max} = g$, 'E' structural material's young module, 'l' length, 'w' width, 't' structure's thickness.

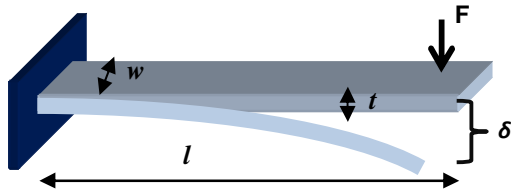


Figure 1: MEMS Cantilever Structure

After substituting the Eq.4, Eq.5 in Eq.3, the 'K', in terms of membrane dimensions is,

$$K = \frac{Ewl^3}{t^3} \tag{6}$$

We can consider the Eq.6, as the cantilever membrane spring constant(K) [1-2].

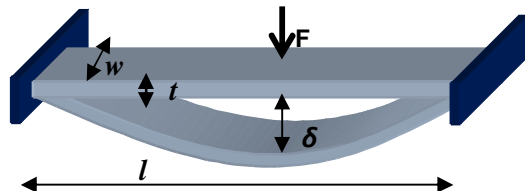


Figure 2: MEMS Bridge Structure

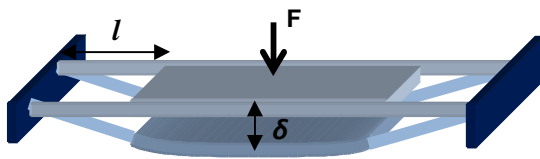


Figure 3: MEMS Clamped-Clamped Structure

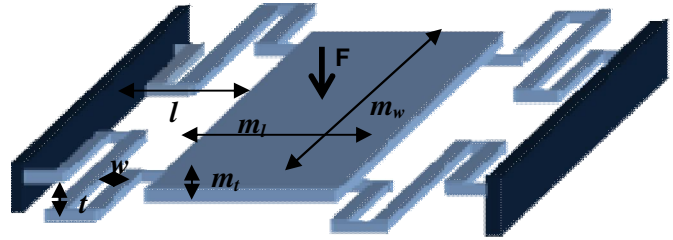


Figure 4: MEMS Serpentine Structure Side View

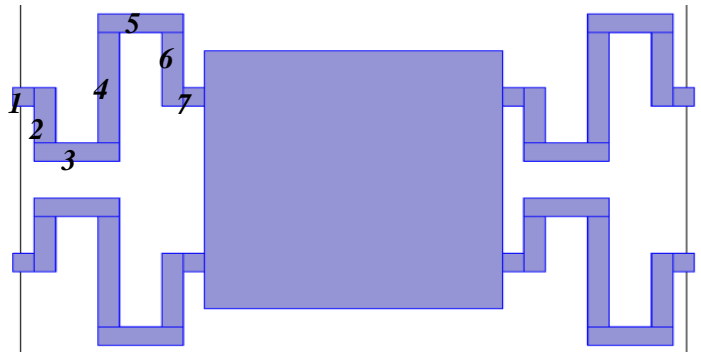


Figure 5: MEMS Serpentine Structure Top View

After doing the analysis on the serpentine structure the spring constant of the structure can be expressed as

$$\frac{1}{K} = \frac{1}{K_1} + \frac{1}{K_2} + \frac{1}{K_3} + \frac{1}{K_4} + \frac{1}{K_5} + \frac{1}{K_6} + \frac{1}{K_7} \tag{7}$$

Where,

$$K_{(1,2,3,4,5,6,7)} = \frac{Ewt^3}{l^3}$$

Table 1: Mathematical Description for membrane Spring Constant[8-12].

Type	Structures	Spring constant in N/m
Cantilever		$\frac{Ewl^3}{t^3}$
Bridge		$\frac{32 Ewl^3}{t^3}$
Clamped-Clamped		$\frac{1.5 Ewl^3}{t^3}$
Serpentine		$\frac{1}{K_{eff}} = \frac{1}{K_1} + \frac{1}{K_2} \dots \frac{1}{K_7}$

We suggest a simpler equation to determine the 'K' of the

clamped-clamped and serpentine structure, i.e., the 'K' of the clamped-clamped and serpentine structure, after a study of the various clamped-clamped structures and serpentine structures[13-17].

$$K = \frac{TEwl^3}{t^3} \tag{8}$$

Here, T is some constant its value we are taken 1.5 for Clamped-Clamped structure, and it will vary in between 0.25 to 0.75 for the serpentine structure.

The mass of the structure depends on the dimensions and the material used, it can be expressed as shown in Eq. 9 for cantilever and bridge structures. But for the clamped-clamped and serpentine structures we need to consider the mass of the rigid body and support legs, but the support legs mass is very less compared to rigid body mass. And the mass of such structure is given in Eq. 10.

$$m = \rho * l * w * t \tag{9}$$

$$m = \rho * m_l * m_w * m_t \tag{10}$$

$$f_r = \frac{1}{2\pi} \sqrt{\frac{K}{m}} \tag{11}$$

Not only did we study the spring constant in this article, but we also created an RF MEMS capacitive shunt switch that is electrostatically actuated with vertical deflection. The output of the switch is calculated primarily by the pull voltage from the Eq. 4 The expression for the structure's voltage pull can be expressed as [18-21].

$$V_p = \sqrt{\frac{8K}{27A\epsilon_0}} (g)^3 \tag{12}$$

3. RESULT ANALYSIS

Overall, four MEMS structures are modeled in this paper, and their spring constant and resonant frequency is measured using the FEM instrument. Finally, using a serpentine MEMS arrangement with perforation, a RF MEMS switch is built at the micro-level. The pull-in voltage is decreased due to the serpentine flexure and the insertion losses are increased with perforation. The focused force on the structures is added to the study of the 'K', and the structure dimensions are shown in Table 1. By applying a DC voltage, all the systems are actuated electrostatically.

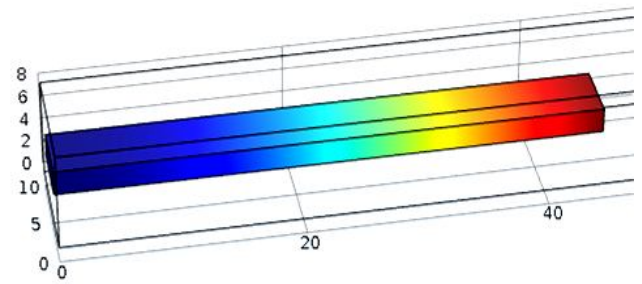


Figure 6: Electrostatically Actuated Cantilever Structure.

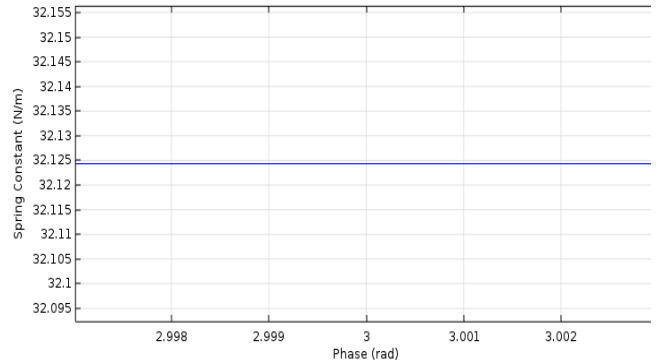


Figure 7: Cantilever Spring Constant.

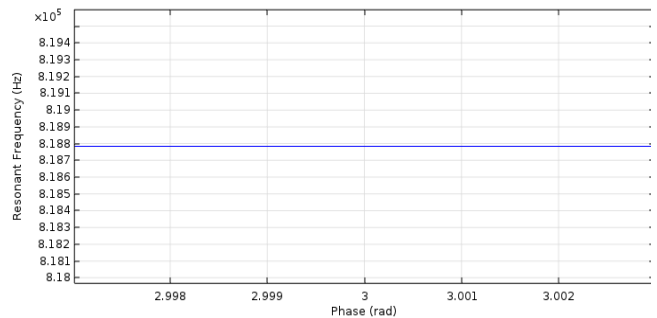


Figure 8: Cantilever Resonant Frequency.

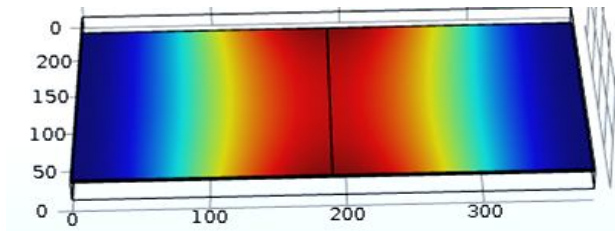


Figure 9: Electrostatically Actuated Bridge Structure.

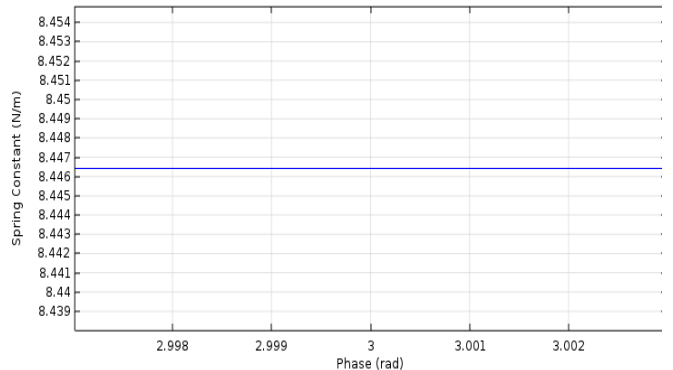


Figure 10: Bridge Spring Constant

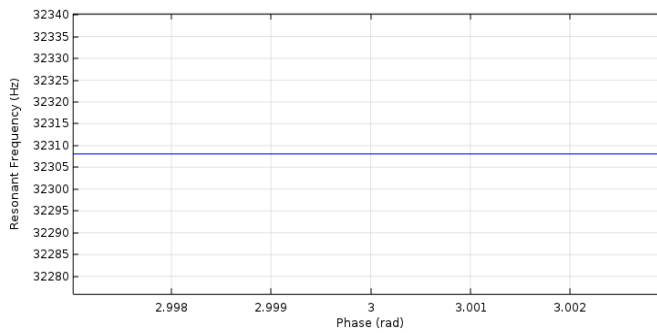


Figure 11: Bridge Resonant Frequency.

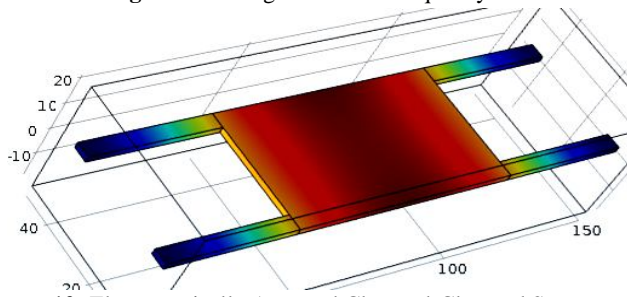


Figure 12: Electrostatically Actuated Clamped-Clamped Structure.

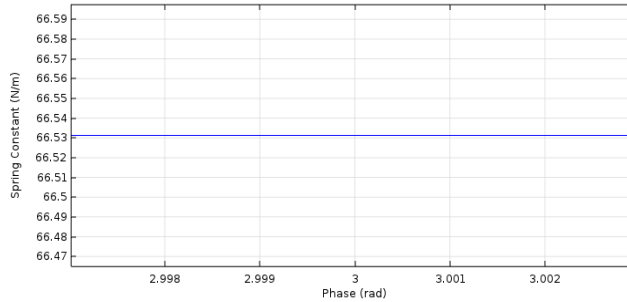


Figure 13: Clamped-Clamped Structure Spring Constant

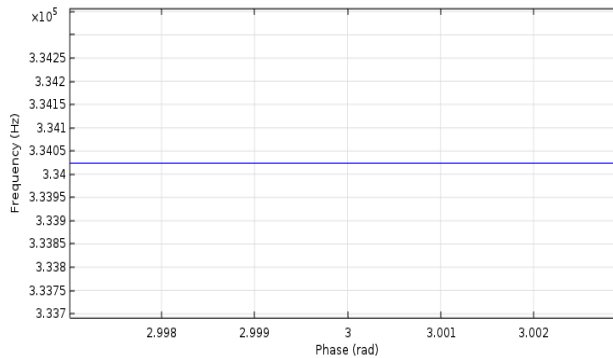


Figure 14: Clamped-Clamped Resonant Frequency.

Table 2: Serpentine Structure Meander Dimensions For Eq.7

Meander Legs	Dimensions in μm ; $w=5$; $t=2$	Spring Constant, K in N/m
1	$l=5$	22400
2	$l=30$	103.7
3	$l=20$	350
4	$l=60$	12.96
5	$l=20$	350
6	$l=40$	43.75
7	$l=5$	22400

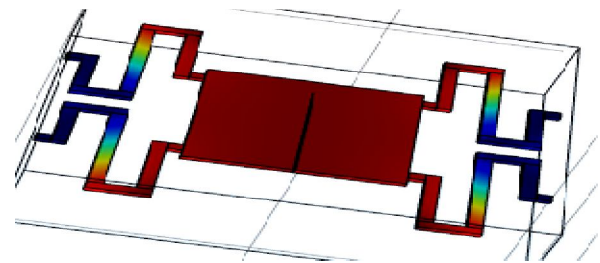


Figure 15: Electrostatically Actuated Serpentine Structure.

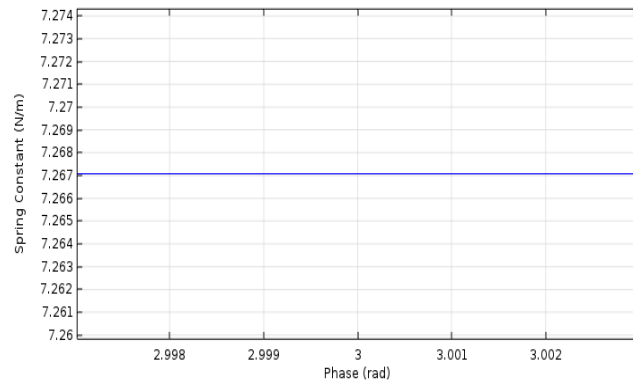


Figure 16: Serpentine Structure Spring Constant

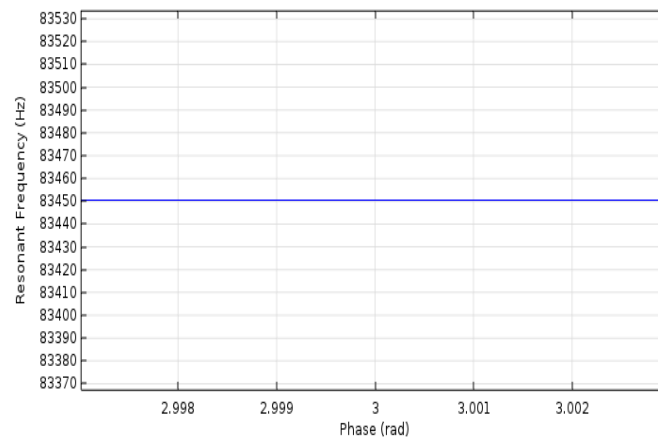


Figure 17: Serpentine Structure Resonant Frequency

Here, in this paper the spring constant of the serpentine structure is calculated with two equations one is existing equation i.e. Eq.7 and other one is the proposed equation i.e. Eq. 8. With the proposed equation we are getting the spring constant for the structure shown in Fig. 15 is 7.68 with T value is 0.25, with the existing equation (Eq. 7) we are getting the spring constant is 8.66. From the simulation we are getting the spring constant of 7.267 as shown in Fig. 16.

In this paper not only the modeling of the spring constant of the MEMS structures, we have designed an RF MEMS switch. The switch is a shunt capacitive and electrostatically actuated vertically deflective type. The switch requiring a voltage of 6.1V for $2\mu\text{m}$ displacement as shown in Fig. 18.

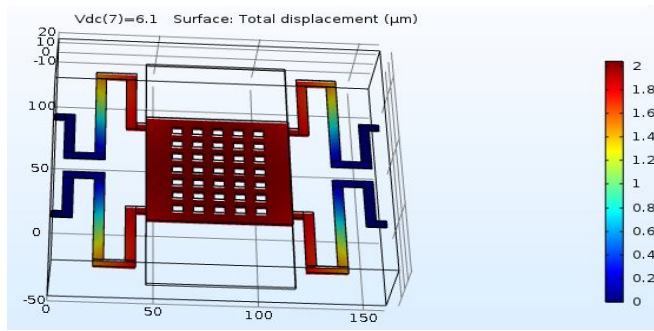


Figure 18: Serpentine Flexure with Perforation, RF MEMS Switch

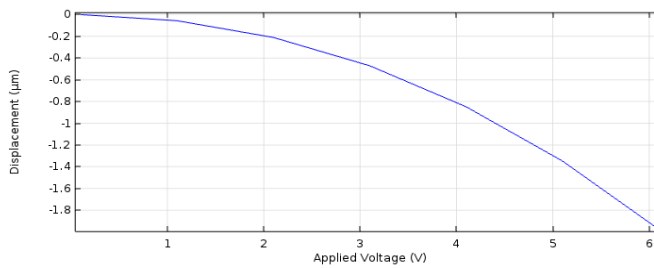


Figure 19: Displacement Vs Applied Voltage

Table 3: Theoretical (Eq.'S Shown In Table I) & Practical Values.

Structure	Dimensions in μm	Theoretical Values [K in N/m, m in Kg, f_r in Hz]	Practical Value [K in N/m, m in Kg, f_r in Hz]
Cantilever	$l=m_l=45,$ $t=m_t=2,$ $w=m_w=5.$	$K=30.73$ $m=1.21 \times 10^{-12}$ $f_r=0.80 \times 10^6$	$K=32.12$ $m=1.21 \times 10^{-12}$ $f_r=0.818 \times 10^6$
Bridge	$l=m_l=380,$ $t=m_t=1,$ $w=m_w=200.$	$K=8.16$ $m=205.2 \times 10^{-12}$ $f_r=0.03175 \times 10^6$	$K=8.445$ $m=205.2 \times 10^{-12}$ $f_r=0.0323 \times 10^6$
Clamped-Clamped	$l=40, m_l=70$ $t=2, m_t=2$ $w=5, m_w=40$	$K=65.6$ $m=15.12 \times 10^{-12}$ $f_r=0.33316 \times 10^6$	$K=66.58$ $m=15.12 \times 10^{-12}$ $f_r=0.33405 \times 10^6$
Serpentine	$l=45, m_l=70$ $t=2, m_t=2$ $w=5, m_w=80$	$K=7.68$ $m=30.24 \times 10^{-12}$ $f_r=0.0802 \times 10^6$	$K=7.267$ $m=30.24 \times 10^{-12}$ $f_r=0.08345 \times 10^6$

As seen in Fig.20, the MEMS structure we have built for the RF MEMS transition has a spring constant of 8.345, and as seen in Fig.21, it has a 0.08943MHz resonant frequency.

The radiofrequency characteristics of the Switch were evaluated using HFSS over the frequency 1GHz-40GHz, and we have found that the engineered switch provides a return loss of -11 dB, insertion losses of -1.2 dB, and insulation losses of -30 dB.

Table 4: Shunt Capacitive Switch Detentions.

Parameter	Value (μm)
Height of the substrate	100
Width of the substrate	400
Length of the substrate	500
Thickness of the Dielectric (t_d)	0.1
Strip Width	70
Width of Electrode	70
Length of Electrode	80
Air Gap (g)	2
Electrodes area ($A=W*w$)	70*80
Bridge Thickness (t)	0.5

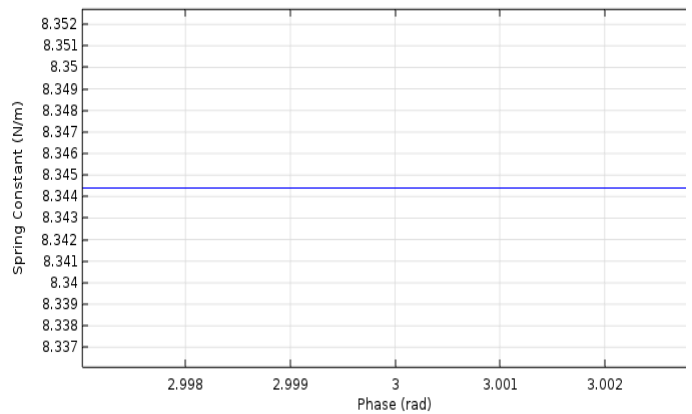


Figure 20: Serpentine Structure with Perforation Spring Constant

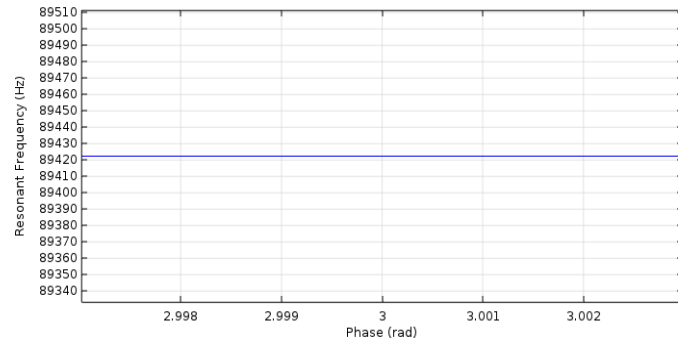


Figure 21: Serpentine Structure with Perforation Resonant Frequency

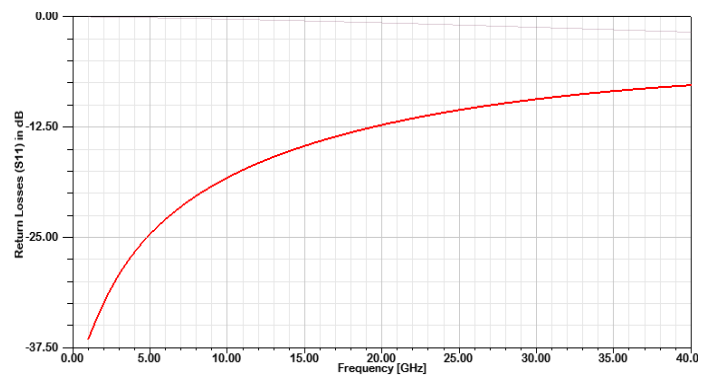


Figure 22: Return Losses (S_{11}) in dB.

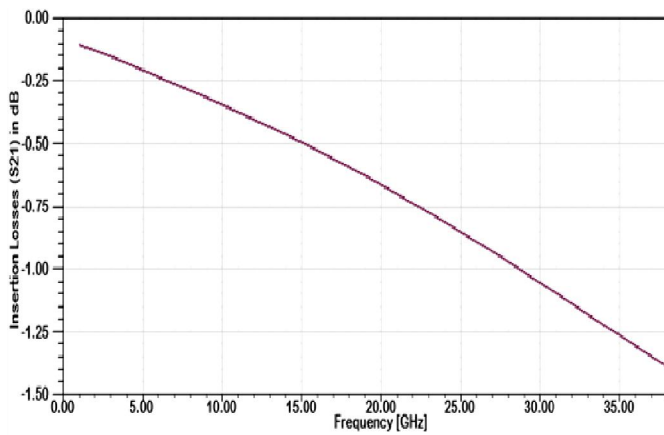


Figure 23: Insertion Losses (S₂₁) in dB

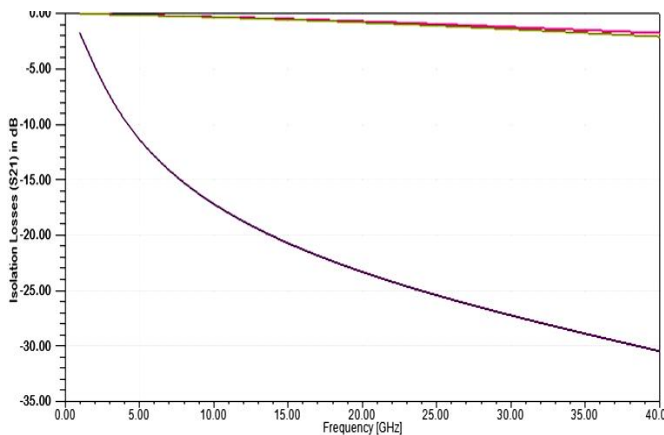


Figure 24: Isolation Losses (S₂₁) in dB

4. CONCLUSION

We modeled, the spring constant (K) of the serpentine MEMS structure in this paper and modeled a RF MEMS transition with a perforation-associated serpentine structure. The switch requiring a voltage of 6.1 V for 2µm displacement. The MEMS structure we developed for the RF MEMS switch has a resonant frequency of 0.08943MHz and has a spring constant of 8.345. The radiofrequency characteristics of the switch were evaluated over the 1GHz-40GHz frequency and we found that the engineered the switch has a return loss of -11 dB, insertion losses of -1.2 dB, and insulation losses of -30 dB.

REFERENCES

[1].Gabriel M. Rebeiz, Jeremy B. Muldavin,**RF MEMS Switches and Switch Circuits**, ISSN 1527-3342/01/\$10.00©2001, IEEE Microwave magazine, Page No.'s:59-71, December 2001.

[2].Viviana Mulloni · BennoMargesin · Paola Farinelli · RomoloMarcelli · Andrea Lucibello · Giorgio De Angelis. **Cycling reliability of RFMEMS switches with Gold-Platinum multilayers as contact material**, DOI

10.1007/s00542-015-2782-2, *MicrosystTechnology*, December 2015.

[3].ParasChawla, Rajesh Khanna. **Design, Analysis and Comparison of Various MEMS Switches for Reconfigurable Planar Antenna**, Acta Polytechnical Hungarica, Vol. 11, No. 10, Page No.:21-40, 2014.

[4].Somayye Molaei, BahramAzizollah Ganji. **Design and simulation of a novel RF MEMS shunt capacitive switch with low actuation voltage and high isolation**", *MicrosystTechnol*, DOI 10.1007/s00542-016-2923-2, 30 March 2016.

[5].Koushik Guha, Mithlesh Kumar, Ajay Parmar, Srimanta Baishya. **Performance analysis of RF MEMS capacitive switch with non uniform meandering technique**, *MicrosystTechnol*, Page No.:2633–2640, DOI 10.1007/s00542-015-2545-0, 2016.

[6].SrinivasaRao. K, Thalluri Lakshmi Narayana. **Review on analytical design, simulation, fabrication, characterization, and packaging aspects of micro electro mechanical switches for radio frequency applications**, *Journal of Bio sensors, Bio Marks, and Diagnostics*, Volume 1-Issue , Page No.:1–6, 2016.

[7].Sean Duffy, Carl Bozler, Steven Rabe, Jeffrey Knecht, Lauren Travis, Peter Wyatt, Craig Keast, and Mark Gouker. **MEMS Microswitches for ReconfigurableMicrowave Circuitry**, *IEEE Microwave and Wireless Components Letters*, Vol. 11, NO. 3. Page No.'s: 106-108, 2011.

[8].Jeremy B. Muldavin, Gabriel M. Rebeiz. **All-Metal High-Isolation Series and Series/ShuntMEMS Switches**, *IEEE Microwave and Wireless Components Letters*, Vol. 11, No. 9, Page No.'s: 373-375, 2001.

[9].DimitriosPeroulis, Sergio P. Pacheco, Kamal Sarabandi,Linda P. B. Katehi. **Electromechanical Considerations in DevelopingLow-Voltage RF MEMS Switches**", *IEEE Transactions on Microwave Theory & Techniques*, Vol. 51, No. 1, Page No.'s: 259-270,2003.

[10].Laurent Dussopt,Gabriel M. Rebeiz. **Intermodulation Distortion and Power Handlingin RF MEMS Switches, Varactors, and Tunable Filters**", *IEEE Transactions on Microwave Theory and Techniques*, Vol. 51, No. 4,Page No.'s:1247-1256, 2003.

[11].Lakshmi Narayana Thalluri, Koushik Guha, K. Srinivasa Rao, **Perforated serpentine membrane with AIN as dielectric material shunt capacitive RF MEMS switch fabrication and characterization**, *Microsystem Technologies*, <https://doi.org/10.1007/s00542-020-04755-3>, 2020.

[12]. Yazan S. Hijazi, Yuri A. Vlasov, and Grover L. Larkins, Jr.**Design of a Superconducting MEM Shunt Switch for RF Applications**, *IEEE Transactions on Applied*

- Superconductivity, Vol. 13, No. 2, Page No.'s: 696-699, 2003.
- [13]. Yazan S. Hijazi, Drayton Hanna, Dane Fairweather, Yuri A. Vlasov, and Grover L. Larkins, Jr. **Fabrication of a Superconducting MEM Shunt Switch for RF Applications**, IEEE Transactions on Applied Superconductivity, Vol. 13, No. 2, Page No.'s: 700-703, 2003.
- [14]. Ari T. Alastalo, Tomi Mattila, Heikki Seppä. **Analysis of a MEMS Transmission Line**, IEEE Transactions on Microwave Theory And Techniques, Vol. 51, No. 8, Page No.'s: 1977-1981, 2003.
- [15]. Brian D. Jensen, Kazuhiro Saitou, John L. Volakis, Katsuo Kurabayashi, **Fully Integrated Electrothermal Multidomain Modeling of RF MEMS Switches**, IEEE Microwave and Wireless Components Letters, Vol. 13, No. 9, Page No.'s: 364-366, 2003.
- [16]. Daniel Saias, Philippe Robert, Samuel Boret, Christophe Billard, Guillaume Bouche, Didier Belot, and Pascal Ancy. **An Above IC MEMS RF Switch**, IEEE Journal of Solid-State Circuits, Vol. 38, No. 12, Page No.'s: 2318-2324, 2003.
- [17]. Dimitrios Peroulis, Sergio P. Pacheco, Linda P. B. Katehi, **RF MEMS Switches With Enhanced Power-Handling Capabilities**, IEEE Transactions on Microwave Theory and Techniques, Vol. 52, No. 1, Page No.'s: 59-68, 2004.
- [18]. David Mardivirin, Arnaud Pothier, Aurelian Crunteanu, Bastien Vialle, and Pierre Blondy. **Charging in Dielectricless Capacitive RF-MEMS Switches**, IEEE Transactions on Microwave Theory and Techniques, Vol. 57, No. 1, Page No.'s: 231-236, 2009.
- [19]. Mandy Axelle Philippine, Hosein Zareie, Ole Sigmund, Gabriel M. Rebeiz, Thomas W. Kenny. **Experimental Validation of Topology Optimization for RF MEMS Capacitive Switch Design**, Journal of Microelectromechanical Systems, Vol. 22, No. 6, Page No.'s: 1296-1309, 2013.
- [20]. Dylan F. Williams, and Roger B. Marks. **Accurate Transmission Line Characterization**, IEEE Microwave And Guided Wave Letters, Vol. 3, No. 8, 1993.
- [21]. Muhua Li, Jiahao Zhao, Zheng You, Guanghong Zhao. **Design and fabrication of a low insertion loss capacitive RF MEMS switch with novel microstructures for actuation**, Solid-State Electronics, Elsevier Publication, Science Direct, DOI: <http://dx.doi.org/10.1016/j.sse.2016.10.004>, 2016.